I.P.N. - 91406 ORSAY CEDEX

institut de physique nucléaire

CNRS - IN2P3 UNIVERSITE PARIS - SUD

IPN

IPNO-DRE 92-27

NUCLEAR DATA FOR UNSTABLE ISOTOPES

O. Sorlin

Institut de Physique Nucleaire, Orsay, France

Invited talk given to the 2nd International Symposium of Nuclear Astrophysics: Nuclei in the Cosmos, Karlsruhe, July 6-10, 1992.

Nuclear Data For Unstable Isotopes.

O Sorlin

Institut de Physique Nucléaire, F-91406 Orsay, France

Abstract. This paper will decribe the ways of producing unstable nuclei in laboratories. The usefulness of the production of unstable species will be emphasized through the major explosive stellar processes.

1. Introduction

Nuclear Physics and Astrophysics are both entrusted with the task of understanding nucleosynthesis and energy production in the stars. At high tempertures and densities present in explosive scenarios such as the early universe, cataclysmic binary stars (nova or accretion stars), and supernovae, the nucleosynthesis proceeds throughout unstable nuclei. In order to produce and to study the most exotic isotopes that are not accessible from stable beam - stable (or radioactive) target experiments, it is necessary to develop facilities that utilize Radioactive Nuclear Beams (RNB).
The existing methods for producing unstable nuclei will be described in § 2. A review of the major explosive stellar processes (inhomogenous big bang (§ 3), rp (§ 4), r (§ 5)) will be made through some selected examples using RNB.

2. Production of unstable isotopes.

Unstable nuclei are produced in laboratories by the "interaction" of a primary beam with a production target. Protons (i), heavy-ions (ii), or neutrons (iii) can be used as primary beams leading to different induced reactions:

(i) spallation, fission and target fragmentation.
(ii) projectile fragmentation, multi-nucleon transfer, fusion-evaporation.
(iii) neutron-induced fission.

The production rate of a Radioactive Nuclear Beam is characterized for all of these methods by the relation:

$$P = \sigma\ I\ N$$

σ is the production cross section in cm^2 which is reaction dependent. I is the intensity of the primary beam in pps, it should be of course as high as possible. N is the target thickness in $atoms.cm^{-3}$. Even if a thick target yields to a high production rate, some compromises will

have to be taken into account in each method for avoiding a (i) too long extraction time of the produced nuclei or (ii) too much energy-losses in the target. The purity of the RNB produced is another important factor for the feasibility of experiments. The two next subsections will describe the two first methods of producing RNB with their corresponding devices for nuclei selection. Further details concerning existing and forthcoming RNB can be found in [1, 2].

2.1 Production of RNB by proton-induced reactions.

A high energy proton beam will produce spallation and fragmentation reactions. If the target nuclei are fissile, a proton or neutron beam can induce fission products. The spallation reaction can be described in two steps: (1) the target nucleus experiences a rapid ejection of nucleons due to the incoming proton and remains in an excited state, (2) it in turn dumps its excitation energy through neutron evaporation. Mainly due to this second step, this method favors the production of neutron deficient nuclei. Conversely, the neutron induced or proton induced fission is more suitable to neutron rich isotopes. The nuclei produced by one of these reactions have to be extracted from the target. Therefore, the target is heated up to 2000 degrees and maintained to a high voltage. Then the reaction products may diffuse in a tube which is at the same voltage. During this process of drifting out of the tube, the reaction products will undergo collisions with the walls, and will thus be ionized by the mechanism of surface ionization. This very simple model of ion-source is limited to the production of isotopes with low ionization potential as Alkaline, Alkaline Earth elements, and Rare Earth. Thus, single charged ions of a well-defined velocity are produced. Due to these features, a magnetic selection will yield to a good selection in Av/Q among the species produced. This method of production is used at ISOLDE/CERN. This method gives high production rates for proton or neutron rich nuclei, and it is at the present time the only way to produce heavy nuclei very far from stability as those encountered in the r process (see §5). Nevertheless, it is important to note the different sources of loss during the ion beam formation as for instance the decay of short-lived species, and the absorption by the tubes during collisions. These losses are shown on Fig. 1.

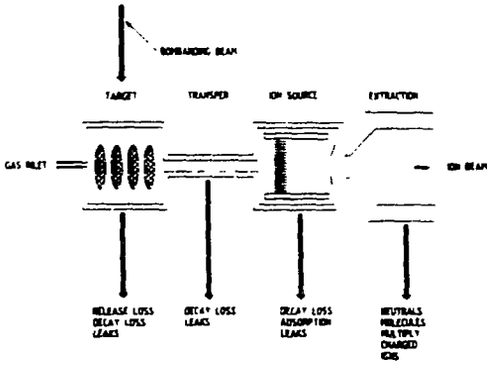

Fig. 1: The steps in the production of an ion beam, with the losses which may occur at each stage [3].

Moreover, the extraction of other species than those mentionned below requires much complicated ion-sources which have to deal with chemical properties of the desired elements. Finally, another selection would be required in order to separate the isobars transmitted by the

magnet. So, even if the production rate is huge, transmission and selection limitations may hamper the production of some desired radioactive species.

2.2 Production of RNB by heavy ion-induced reactions.

Three different kind of reaction can occur depending on the energy of the incident projectile. At high energies (>200 MeV/u), a pure fragmentation of the projectile will happen. These energy domains are used for instance in Berkeley, GSI, Saturne facilities. This method will produce elements ranging from the lightest up to the beam mass. The fragmentation can be described as following by the so called Participant-Spectator Model: once the projectile collides with the target, parts of the projectile and target form a highly excited participant which travels at an intermediate energy between velocity of the target and of the beam.The remaining part of the target form the so called target spectators, whereas the remaining parts of the projectile still travel focused around the beam incident direction and with the beam velocity. At intermediate energies (between 30 and 100 MeV/u) like in GANIL, MSU, RIKEN facilities, some multi-nucleons transfers also occur (see for instance §5 which shows up the prossibility of producing ^{46,47}Cl with a ^{48}Ca beam). Due to this exchange possibility between projectile and target, a high (resp. low) N/Z ratio of the target will enhance the production rate of neutron (resp. proton) rich nuclei. At energies just above the coulomb barrier, fusion evaporation reaction lead to the production of specific species by the appropriate choice of projectile and target. In the fragmentation process, thick target are important for increasing the reaction rate. Nevertheless, this target thickness is limited because of slowing down, angular and energy stragglings of the fragments in the material. These interactions degrade the narrow velocity and angular distibutions of the fragments. These beam qualities are required for guiding the fragments into a spectrometer. This spectrometer, used for the selection of nuclei of interest, is generally composed with three parts which are: the magnetic, the degrader, and the velocity selections. This is sketched on Fig. 2 where the F1-3 slits account for the three selections.

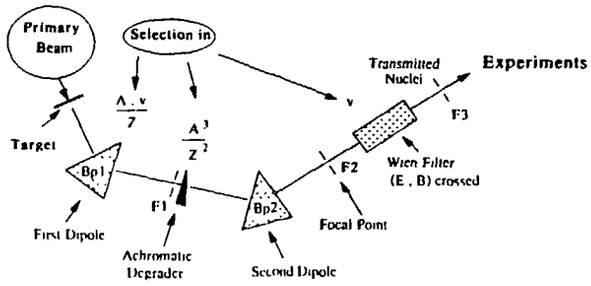

Fig. 2: Schematic view of a spectrometer composed with three selections (magnetic, energy-loss, velocity).

The first magnet deflects the fragments according to the relation $B\rho = Av/Z$ (for fully stripped ions). The degrader is a layer of material that induces different energy-losses for each element. According to the Bethe approximation $dE/dx \propto AZ^2/E$, each nucleus of energy proportional to Z^2/A after the first magnet will loose $dE/E \propto A^3/Z^2$. The magnetic field of the second dipole has then to be matched to the output energy of the desired nucleus. It will be then preferentially transmitted. The third selection can be performed by a velocity filter, composed with electric

and magnetic crossed fields. The nucleus whose velocity is equal to $(E/B)_{filter}$ will travel straightforward, others will be deflected. An example of the efficiency of these three sets of selections is shown below (Fig. 3) in the case of the fragmentation of ^{24}Mg for producing a ^{20}Mg secondary beam.

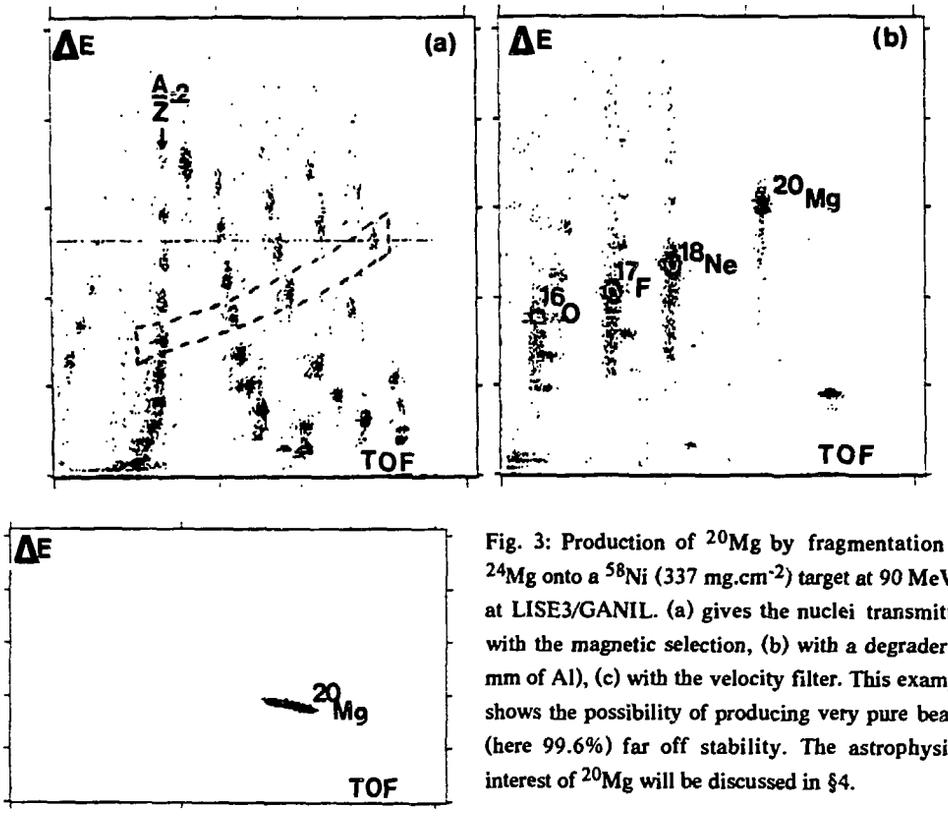

Fig. 3: Production of ^{20}Mg by fragmentation of ^{24}Mg onto a ^{58}Ni (337 mg.cm^{-2}) target at 90 MeV/u at LISE3/GANIL. (a) gives the nuclei transmitted with the magnetic selection, (b) with a degrader (1 mm of Al), (c) with the velocity filter. This example shows the possibility of producing very pure beams (here 99.6%) far off stability. The astrophysical interest of ^{20}Mg will be discussed in §4.

This fragmentation method is well suited for the production and selection of light species on the proton or neutron rich side (see §3, 4, 5). Actually, at intermediate energies, the production of unstable nuclei is limited to masses lower than ≈ 100 due to the production of charge states in the target at these energies. This effect will considerably hamper the discrimination of the fragments produced. The drawbacks of the fragmentation method are different in the case of high or intermediate energy incident beam. At the present time, high energy facilities which do not encounter charge states problems, unfortunatly have two low primary intensities to reach species very far of stability.

3. Inhomogeneous big-bang nucleosynthesis

The standard big-bang nucleosynthesis model is known to reproduce fairly well the abundance of nuclei up to (A=7, Z<4), but cannot bridge the A=5 and A=8 gaps. Therefore, it cannot account for the production of heavier nuclei. Inhomogeneous scenarios, which are characterized by a nonuniform density of the universe, may overcome this problem by

successive neutron and α captures leading to higher masses. Recent measurements in the region of ^{8}Li have been performed in order to quantify the light element production. The important reactions that are thought to occur in this region, and through which all nuclides of mass A>11 must pass (in this kind of scenario) are represented on the Fig. 4. Recent experiments have been performed in Japan [4] and in the USA [5] with a ^{8}Li radioactive beam, measuring the reaction rates of ^{8}Li(α,n)^{11}B, ^{8}Li(d,n)^{9}Be and ^{8}Li(d,t)^{7}Li respectively. The first experiment shows an enhancement of this reaction rate of a factor of five as compared to inverse reaction measurement [6], due to the fact that the inverse reaction only proceeds through the ground state of ^{11}B. This factor will probably increase the production of intermediate mass element and thus strengthen the occurence of this inhomogeneous scenario.

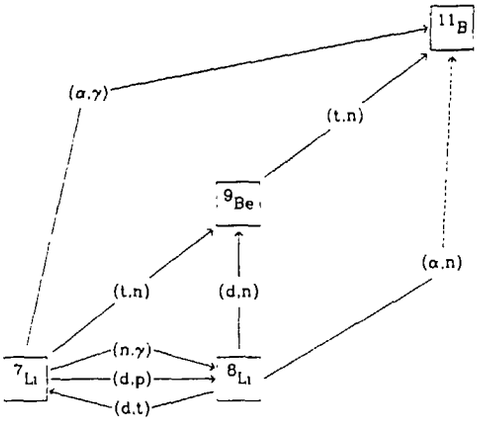

Fig. 4: Major reactions and pathways relevant for the synthesis of ^{8}Li, ^{9}Be, ^{11}B and for the building of heavier species with primordial inhomogeneous nucleosynthesis [5].

4. From the hot CNO cycle to the rp process

Although of minor importance for the synthesis of the element in the universe, processes involving proton captures are often important for explaining the nuclear energy production in stars. A comprehensive review of the explosive proton capture scenarios can be found in [7] and in the included references. In main sequence stars, the nuclear burning of hydrogen (pp chains and CNO cycle) accounts for the energy production that matches the gravitational shrink and converts H into He. At temperatures and densities much higher than those encountered in such star's interior, the hot CNO cycle (HCNO) will increase the energy generation including the ^{13}N(p,γ)^{14}O reaction. At much higher temperatures of about T_8 =2 (2.10^{8}°K) several breakout reactions may happen leading to other cycles due to the bypass of the long-lived nuclei ^{14}O, ^{15}O (half-life respectively 102s and 176s). The ^{15}O(α, γ)^{19}Ne and ^{19}Ne(p, γ)^{20}Na reactions are supposed to generate a way of escape towards higher masses (about A=70). The so-called rp process is then driven by the competition of rapid proton captures and β^{+} decays (Fig.5). While the β^{+} decay rates are not sensitive to an increasing temperature, the proton capture rates increase exponentially, yielding to a reaction flow more or less far off stability depending of the temperature conditions (T_8 > 2). The reaction rates for the different capture reactions have to be known to predict the reaction path for different

temperature and density conditions, to determine the resulting isotopic abundances, and to evaluate the nuclear energy production and the time scale of the process. High temperature and density conditions may occur in a large variety of astrophysical sites like cataclysmic binary systems (including novae and some X-ray bursts), and during type II supernovae explosions. The former objects are thought to be thermonuclear outbursts triggered by mass accretion onto the surface of either a white dwarf or a neutron star. The nuclear reactions are therefore critical for the understanding of the outburst phenomenon itself together with the concommitent synthesis of elements. Even if it seems, up to now, beyond the edge of feasibility, the estimated isotopic abundances deduced from an rp reaction network calculation would lead to an extremely interesting comparison with the rate of γ-ray emission of characteristic long-lived isotopes (^{22}Na, ^{26}Al, ^{44}Ti, ^{54}Mn, ^{56,57}Co, ^{65}Zn) detected by the Gamma Ray Observatory. It could also be of great interest for the understanding of some isotopic anomalies observed in primitive meteorites, as for instance the overabundance of ^{26}Mg.

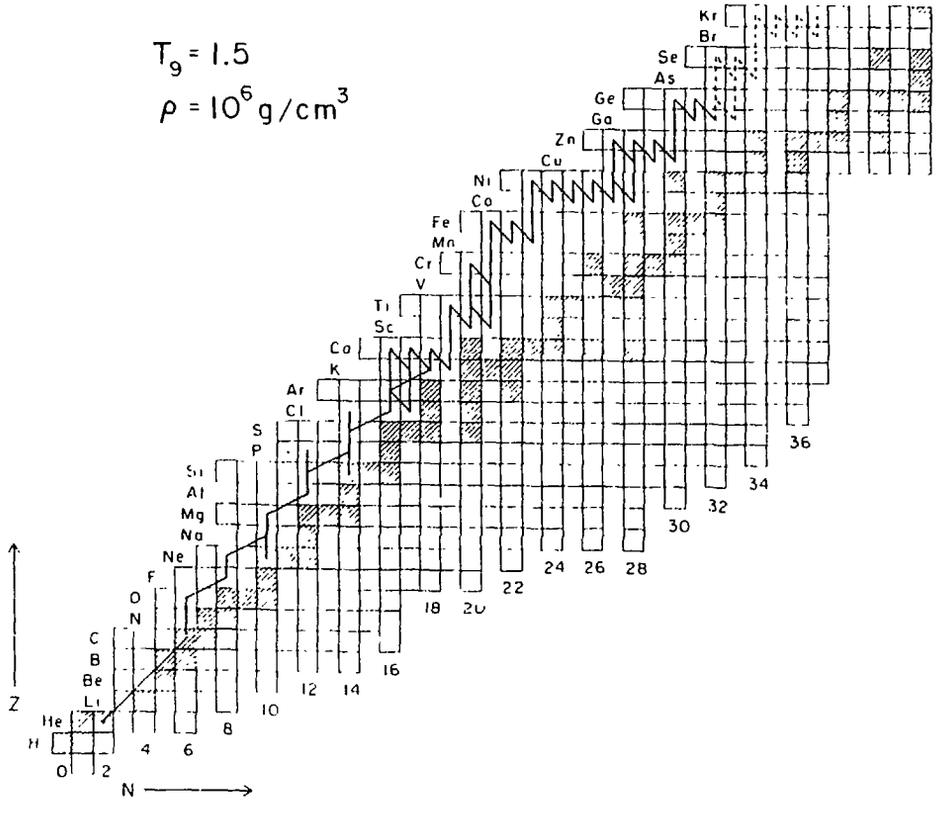

Fig. 5: Major flows in the rp process are indicated with solid arrows. The dashed arrows account for a flow of less than 1/10 of the solid arrows [7].

Because reaction cross sections at stellar energies are often extremely low, it is scarcely possible to measure the direct reaction rate in the laboratory. Nevertheless a first step has been made in Louvain-la-Neuve facility for the ^{13}N(p, γ)^{14}O reaction by means of a low energy and high intensity beam of ^{13}N. Generally, for light species, the reaction rate is dominated by the resonant term. In the case of the ^{19}Ne(p, γ) ^{20}Na reaction, it is proportional to:

$$\lambda p\gamma\,(^{19}Ne) \propto T_9^{-3/2} \sum_r \omega\,(J(^{19}Ne), J_p, J_r)\,\frac{\Gamma p\,\Gamma\gamma}{(\Gamma p + \Gamma\gamma)} \exp\,(-\,11.60045\,E_r(MeV)/T_9),$$

where Γ_p, and Γ_γ are the proton and the gamma widths respectively which characterize the formation and the decay of the compound nucleus $^{20}Na^*$, and ω is the statistical factor. This reaction rate cannot, at present time, be deduced from a direct reaction. Though indirect measurements allows to determine the position of the energy resonances in ^{20}Na. As shown in figure 6, it is of utmost importance for the knowledge of the temperature onset of the rp process. The left curve [8] shows that (taking theoritical estimates of the Γ widths and the spin parities) the determination of the resonant energy yields to a breakout temperature of about $T_8 \approx 2.2$, instead of $T_8 \approx 3.8$ deduced by Langanke [9] from the level properties of the mirror nucleus ^{20}F.

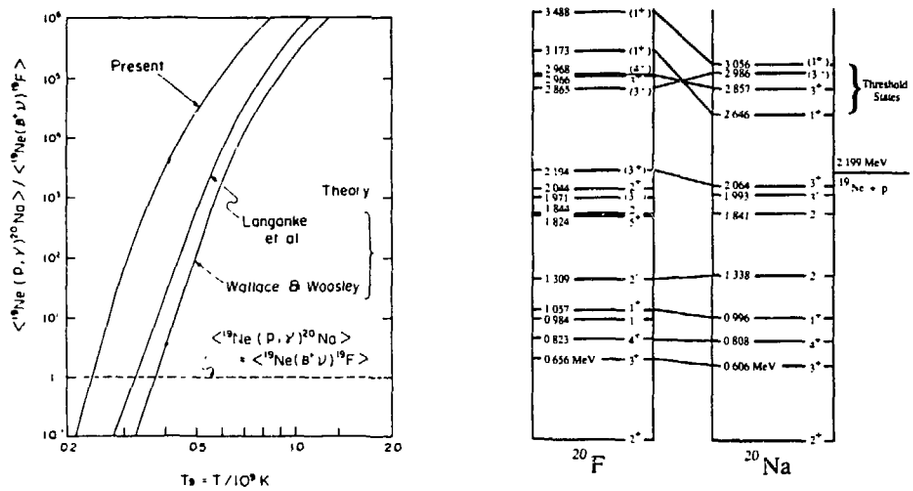

Fig. 6: The left part [8] shows the ratio of proton capture $^{19}Ne(p,\gamma)^{20}Na$ reaction against the decay to ^{19}F. The calculation has been made by different authors who took into account the energy levels of the mirror nucleus (Wallace & Woosley [10]), the predicted Thomas-Ehrmann shift to the excited states of ^{20}Na (Langanke et al. [9]). The experimental determination of these energy levels (right part) [8, 11, 12, 33] by transfer reaction leads to a huge increase of the ratio (named "Present" [8]), and thus a lower escape temperature from the HCNO cycle.

These level positions have been experimentally determined by the transfer reaction $^{20}Ne(^3He, t)^{20}Na$ [8, 11, 12]. They are very different from the predictions of Langanke (Fig. 6). This strengthens the necessity of such measurements. The most important levels are those in the Gamow peak region for the temperature of interest. The 2.646 MeV which is thought to be a 1^{+} or 0^{-} state seems to be the most promising level above the proton threshold. The observation of the delayed protons and γ rays from ^{20}Mg (Fig. 7) and their relative ratios determine whether this first level of ^{20}Na (above the proton reaction threshold) could enhance the reaction rate. Figure 7 shows an example of an experiment performed at GANIL looking at the β^+ decay of ^{20}Mg through p-γ coincidences in order to correlate the protons from the $^{20}Na^*$ with the excited states of ^{19}Ne. The results from this experiment are preliminary and are presently under further analysis to extract the astrophysically interesting information [13].

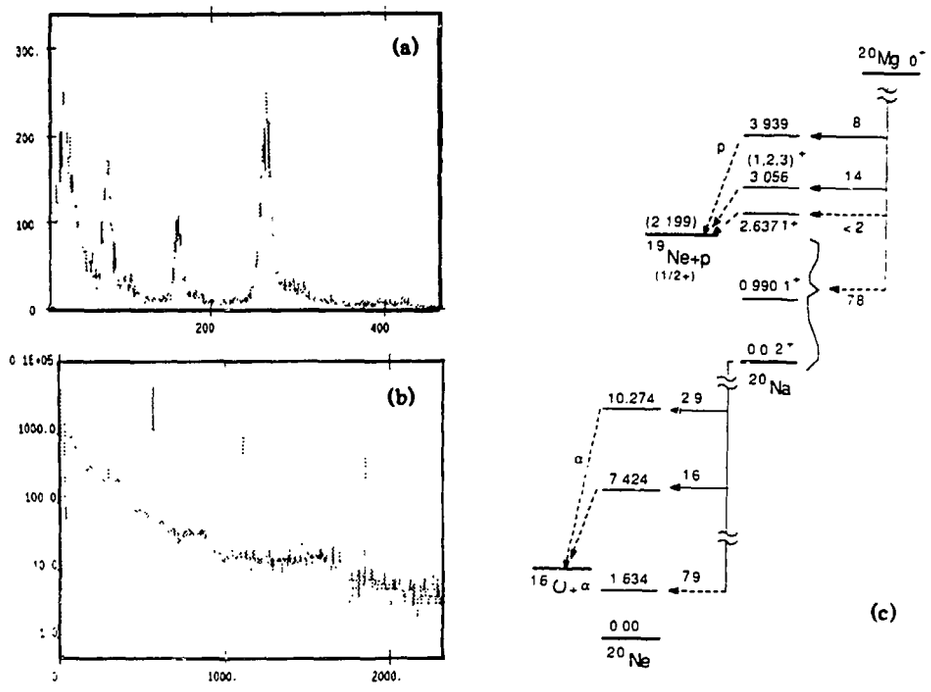

Fig. 7: The on-line proton (a) and the gamma spectra (b) of ^{20}Mg decay (see Fig. 3 for its production) have been obtained in coïncidence with a β ray in order to avoid major parts of background. The corresponding level scheme and branching ratios (c) [14], partially known before the experiment will be improved by the present much important statistics, and the possible correlation between protons from ^{20}Na* and γ rays from ^{19}Ne* may be discovered [13].

The capture reaction flow to higher masses will be hindered by photodesintegration processes for low S_p-value nuclei and then will have to wait for the β-decay of the latter. The reaction rates close to the proton drip line or near closed shells (low S_p-values) can be determined by single resonances because of the low level density above the proton threshold. Thus, in some selected cases (low S_p-values, light nuclei) the precise determination of the resonance parameters is required. In the high mass region, not only the reaction rates are unknown, but also even the nuclear properties as β^+ decay, masses, deformations... Many experiments are pionneering these "exotic" regions. For instance, some nuclei have been recently identified (^{43}Cr, ^{46,47}Fe), and some half-lives and level schemes determined at LISE3/GANIL (see for instance the example of ^{31}Ar in Fig. 8 and [15] for the study of the $23 < Z < 26$ region). These level schemes experiments, devoted to the study of the β-p-γ decays of very unstable nuclei as ^{31}Ar (shown in Fig. 8) may give wealthy information on the Γ_p / Γ_γ ratios of the β-decay populated excited states above the proton threshold of the daughter nucleus (here ^{30}S). This kind of method could be used for the indirect study of proton capture rates on nuclei involved in the rp process path.

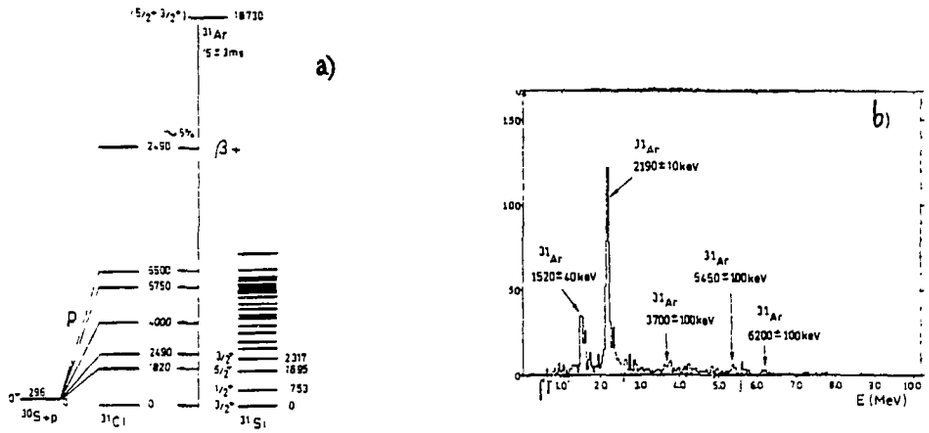

Fig. 8: Example of a part of the decay scheme of ^{31}Ar (a) taken from [16] with the corresponding proton energy spectra (b). This shows that a determination of the level schemes of very proton-rich nuclei is feasible even if it is located at the drip-line.

The investigations in the region of ^{65}As at NSCL / MSU, necessary for the knowledge of predicted bottelneck nuclei, are presented on figure 9.

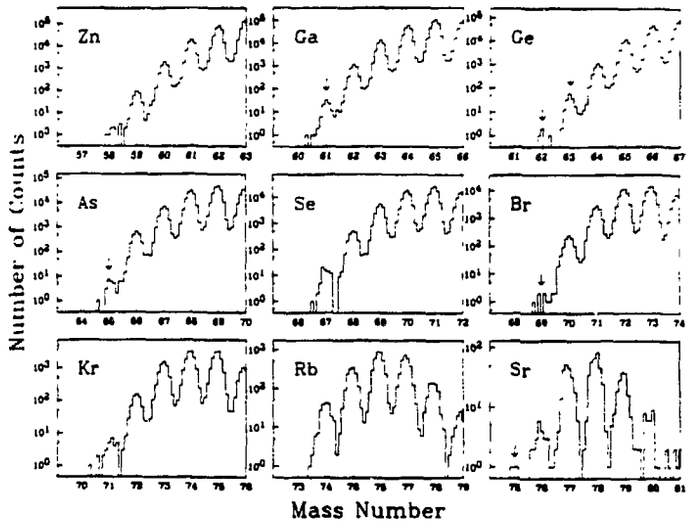

Fig. 9: Mass spectra observed for some elements observed among the ^{78}Kr fragmentation products. The newly discovered nuclei are indicated by the arrows [17]. The observation of ^{65}As and of ^{69}Br, hitherto predicted unbound, shows that the rp process can proceed through these nuclei. Conversely, the non-observation of ^{73}Rb will probably delay this process for reaching higher masses.

So, according to the production rate in the rp process path, it may be possible to study some important nuclear parameters as for instance the masses or the level scheme. These properties are necessary to refine the statistical Hauser-Feshbach calculations of the reaction rates for the

nuclei which exhibit a high level density at the reaction threshold. Then, the parameters for the formation and the de-excitation of the compound nucleus are required (for A+p → B* → B+γ). This includes: mass determination, level densities, mean Γ_p, the knowledge of the low energy levels in the B nucleus, and the level strengths by Giant Dipolar Resonance properties.

5. The neutron rapid captures processes.

The r process is known to synthesize about half of the elements heavier than iron. Its contribution is deduced from the predicted s process element abundance [18]. (The study of the s process lies beyond the scope of this review which deals with explosive processes). After about 30 years of efforts devoted to the knowledge of a most "plausible site for the r-process ([19])" and to explain the observed abundance curve of the elements, very recent improvements seem to show that a major step is occuring. A comprehensive review of the r process can be found in [20]. The r process is thought to develop in the hot bubble formed during a supernova (SN) explosion ([19] and references herein). The observational data suggest that low-mass type II SN may be the most likely contributors to the r elements [21]. However, less extreme conditions of density and temperature could produce rapid neutron captures. These conditions are encountered in the He layers of SN, the neutron flux being released by explosive (α, n) reactions on ^{13}C, ^{22}Ne induced by the passage of the shock wave of the explosion. The "classical" r process path drives far off stability by successive neutron captures and β^- decays (Fig. 10). The neutron capture is impeded by the photodesintegration when the path reaches neutron closed shells (because of the low S_n encountered) and have to wait until the β decay of the nucleus. These nuclei, at the different neutron closed shells N = 50, 82 and 126 are the classical "waiting points". An (n, γ)-(γ, n) equilibrium is reached for high temperature and density conditions. Thus, if we can determine the neutron separation energy S_n, the neutron density d_n and the stellar temperature, the abundance of these unstable progenitors is simply given by the Saha equation:

$$N(A,Z) \propto N(A-1,Z)\ \frac{d_n}{T^{3/2}}\ \exp\left(\frac{-S_n}{kT}\right)$$

The enhancements in the r element abundance curve (see insert in Fig. 10) called "r peaks" are evidences of the accumulation time at these waiting points. The understanding of the position and of the isotopic abundance ratios around these peaks is clearly related to the knowledge of the decay properties (half-life $T_{1/2}$ and neutron-delayed emission probability P_n) of nuclei around the closed shells. The measurements of these key properties by Kratz et al. allows to fix constraints upon the neutron capture time (and then on the neutron density d_n)and on the temperature necessary to match the β decay rates. The experimental work at ISOLDE / CERN concerning the waiting point nuclei $^{130}Cd_{82}$ and $^{79}Cu_{50}$ [26, 32] brings substantial informations about the conditions of temperature and neutron density required into stellar environment to exhibit an r process. An imaging picture of the correlation between the progenitors and the stable r process elements at the N = 130 closed shell, shown on Fig. 11.

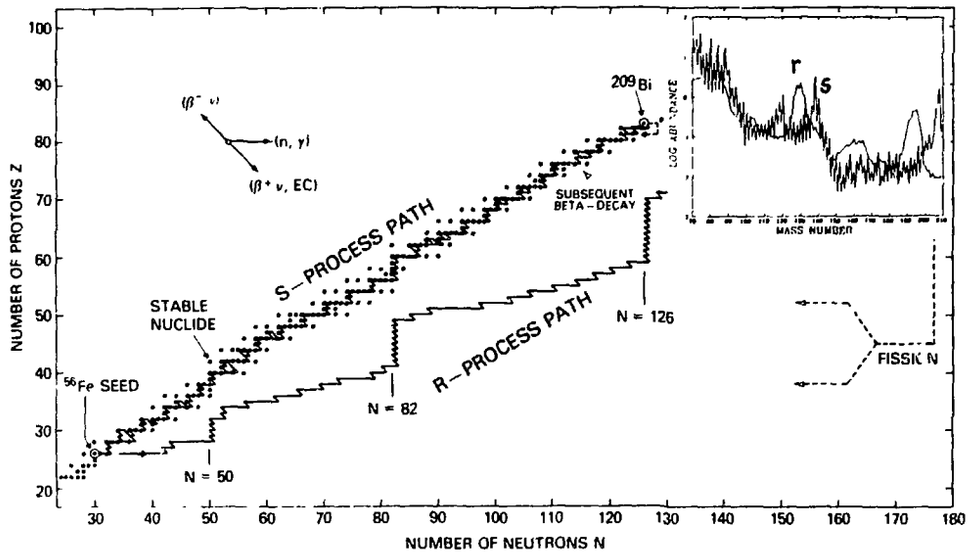

Fig. 10: Schematic view of the r process path in the (N, Z) plane [22]. This path was computed for a temperature of $T_9 = 1$ and a neutron density $d_n = 10^{24}$ n.cm^{-3}. The r process element abundance curve deduced from the estimated s process is presented in the insert.

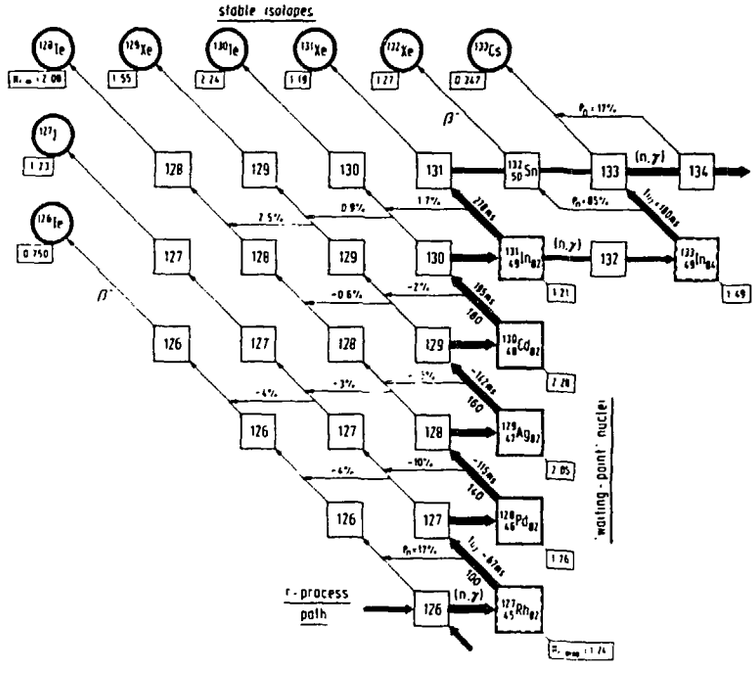

Fig. 11: Schematic view of the r-abundance features and the β-decay properties of nuclei in-or-close to the r process path in the A = 130, "waiting point region" [26]. $T_{1/2}$ and P_n values given in this figure are either experimental values ($^{131, 133}$In, ^{130}Cd) or RPA predictions.

Recent calculations including these measurements and high quality predictions for nuclear masses and β decays, show that the three peaks cannot be fitted by a global steady flow calculation, but at least three different neutron densities have to be included. Thielemann and Kratz [23, 24] point out that additionnal experimental data (masses, $T_{1/2}$, P_n, deformations, level schemes) far off stability as well as theoretical improvements are needed to obtain good agreement not only for the peaks but also for the whole abundance curve of the r elements. It seems that some discrepancies between the fitted and observed curve may reflect nuclear structure as for instance the transition from deformed to near spherical isotopes in the r process path before the neutron closed shells. Preliminary experiments have been performed in the Fe region at FRS / GSI and ILL [25]. Even if the predicted branching points (by β decay) are still out of reach, this is a first step to the study of this region.

The r process is historically related to neutron captures on an iron seed. But, as mentioned above, these neutron captures can also occur for lighter species produced by either the photodesintegration of iron in the α process model [27] or in He burning shells on "seed" nuclei. Anyway, a kind of r process has to be invoked to explain the existence of light stable neutron-rich isotopes as ^{46,48}Ca.

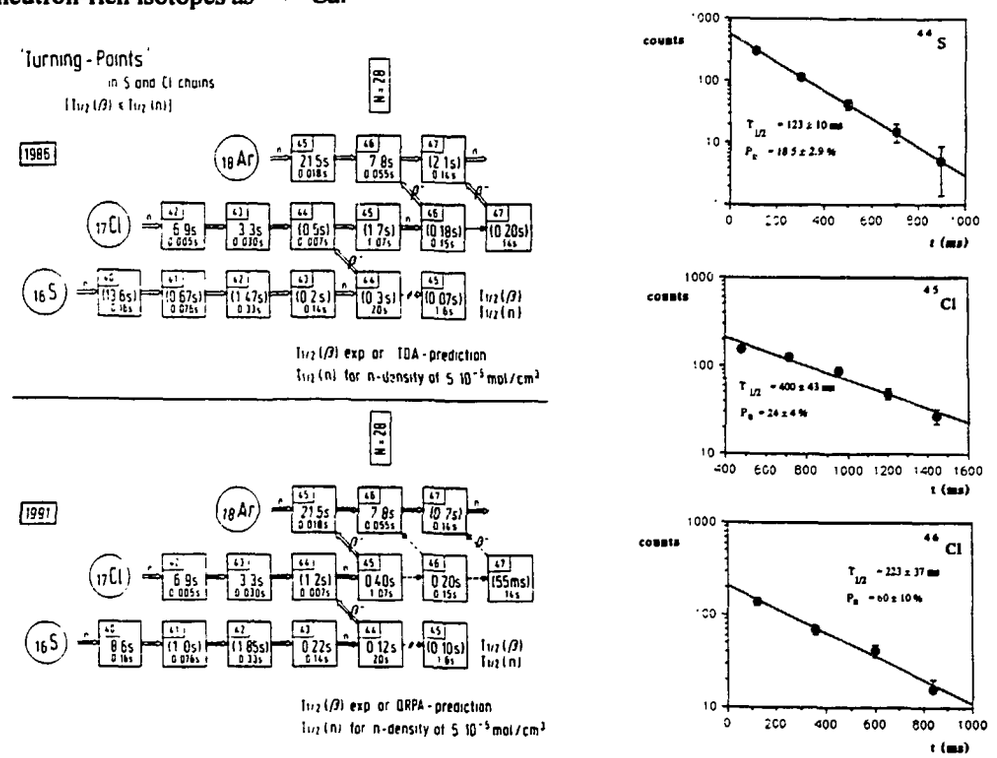

Fig. 12: Neutron capture path in the $_{16}$S to $_{18}$Ar chains for a stellar temperature of 8 Tg and a neutron density of 5 10^{-5} mol cm^{-3}; upper part: status in 1986, lower part: present status. With the new experimental data obtained at LISE / GANIL facility [31], at both N = 28 "turning points" isotopes, ^{44}S and ^{45}Cl, β-decay starts to dominate over further neutron captures. Hence, the possible A= 46, 47 progenitors of ^{46}Ca will be produced in small amounts only. Even if the neutron capture path reaches ^{46}Cl and ^{47}Cl, their respectively higher and lower P_n-values largely contribute to the reduction of ^{46}Ca production. With this, large ^{48}Ca/ ^{46}Ca ratios can be obtained, as required to explain the observed abundances in EK-1-4-1 inclusion [28]. The right part shows the experimental data.

In fact, neither O and Si burning nor the s process can reach such neutron rich nuclei. In order to understand their synthesis and their abundance ratio, which has been found to be 50 in the solar system and 250 in refractory inclusions of the Allende meteorite, the decay properties of their progenitors have to be determined. Actually, the theoritical predictions cannot hold for such an underabundance of ^{46}Ca without invoking very severe stellar constraints on the neutron exposure [28, 29]. ^{46}Ca was thought to be produced mostly by the decay of ^{46}Cl (Pn = 30%) and of ^{47}Cl (P_n = 100%) (Fig. 12). The most striking effect given by the experimental results (shown in Fig. 12 right part) is the much shorter half-life of ^{45}Cl compared with the predictions. This nucleus then acts as a turning point and drives the path preferentially towards ^{45}Ca. The contribution of the A = 46,47 progenitors of ^{46}Ca will then be reduced (see caption of Fig. 12). It is important to note that the observed overabundances of ^{48}Ca, ^{50}Ti and ^{54}Cr seem to be correlated with those of ^{58}Fe, ^{64}Ni, ^{66}Zn [30]. Hence, astrophysical models have to show how they can produce all correlated abundances in a realistic and selfconsistent way. This emphasizes the growing complementarity between nuclear physics and isotopic anomalies observation.

Conclusion:

Nuclear Physics plays a key role in the understanding of the origin of the elements in nature and in the energy production in stars. Explosive stellar processes require the knowledge of nuclear properties of very far off stability species. Therefore, RNB facilities are necessary for their study. It has been widely outlined that experiments are successfully being performed on each side of the valley of stability. Though, improvements need to be achieved to cover a broader range of nuclei along explosive nucleosynthesis paths. RNB projects, as it is shown in [1, 2, 34] are promising and set excitements in the nuclear astrophysicists community.

Acknowledgments:

I would like to adress special thanks to D. Guillemaud Mueller, K.-L. Kratz, M. Mohar, A. C. Mueller and M. Wiescher for their fruitful comments and discussions concerning this work.

References:

[1] 1989 *Proceedings of the First International Conference on Radioactive Nuclear Beams, October 16-18, Berkeley, ed. Nitschke J M.*
[2] 1991 *Proceedings of the Second International Conference on Radioactive Nuclear Beams, Louvain-La-Neuve, August 19-21, ed. Adam Hilger.*
[3] Ravn H L and Allardyce B W 1989 *Treatise on Heavy-Ion Science, Vol. 8, ed. Bromley D A, Plenum Press New York* p. 363.
[4] Boyd R N et al. 1991 *Nucl. Phys. A* 538 523c.
[5] Farrel et al. 1991 *Proceedings of the Second International Conference on Radioactive Nuclear Beams, Louvain-La-Neuve, August 19-21, ed. Adam Hilger* p. 287
[6] Paradellis T et al. 1990 *Z. Phys. A* 337 211.

[7] Champagne A E, Wiescher M 1992 *Ann. Rev. of Nucl. and Part. Sci.* in print.
[8] Kubono S et al. 1989 *Ap. J* **344** 460, Kubono S 1988 *Z. Phys. A* **331** 359.
[9] Langanke K et al. 1986 *Ap. J* **301** 629.
[10] Wallace R K and Woosley S E 1981 *Ap. J Suppl.* **45** 389.
[11] Lamm L O et al. 1990 *Nucl. Phys. A* **510** 503.
[12] Smith M S et al. 1992 *Nucl. Phys. A* **536** 333.
[13] Piechaczek A et al. 1992 *Proceedings of the 6 th Conference on Nuclei far from Stability, 19-24 July, Bernkastel-Kues* to be published.
[14] Kubono S et al. 1991 *Proceedings of the Second International Conference on Radioactive Nuclear Beams, Louvain-La-Neuve, August 19-21, ed. Adam Hilger* p. 317.
[15] Borrel V 1992 *Z. Phys.* to be published.
[16] Borrel V et al. 1987 *Nucl. Phys. A* **473** 331, see also Bazin D et al. 1992 *Phys. Rev. C* **45** (1) 69.
[17] Mohar M et al. 1991 *Phys. Rev. Lett.* **66** (12) 1571.
[18] Käppeler F 1989 et al. *Rep. Prog. Phys.* **52** 945.
[19] Meyer B S et al. 1992 *Proceedings of the Origin and Evolution of the Elements, June 22-25, Paris, to be published in Cambridge Univ. Press* and submitted to *Ap. J.*
[20] Cowan J J and Thielemann F-K 1991 *Phys. Rep.* **208** 267.
[21] Mathews G J and Cowan J J 1990 *Nature* **345** 491.
[22] Rolfs C E and Rodney W S 1988 *Cauldrons in the Cosmos, ed. Univ. of Chicago Press.*
[23] Kratz et al. 1992 *Contribution to this Conference.*
[24] Thielemann F -K and Kratz K -L 1991 *Proceedings of the 22nd Mikolajki Summer School, Selected topics in Nuclear Astrophysics, ed. Szeflinska G, IOP Publishing, Bristol.*
[25] Czajkowski et al 1992 *Contribution to this Conference.*
[26] Kratz K-L 1988 *Rev. in Mod. Astron.* **1** 184, Kratz et al. 1991 *Proceedings of the International Workshop on Nuclear Shapes and Nuclear Structure at low excitation energy, Cargèse, June3-7.*
[27] Woosley S E and Hoffman R 1991 *Ap. J.* in print.
[28] Kratz K-L et al. 1991 *Proceedings of the First European Biennal Workshop on Nuclear Physics, March 25-29, Megève, ed. World Scientific.*
[29] Thielemann etal. 1990 *Proceedings of the International Symposium on Nuclear Astrophysics, Nuclei in the Cosmos, June 18-22, Baden/Vienna, ed. Oberhummer H and Hillebrandt W.*
[30] Harper C L et al. *Proceedings of the International Symposium on Nuclear Astrophysics, Nuclei in the Cosmos, June 18-22, Baden/Vienna, ed. Oberhummer H and Hillebrandt W.*
[31] Sorlin O 1991 Thèse de l'Université Paris VII, IPNO -T.91.04.
[32] Kratz et al. 1992 *Ap. J.* to be published.
[33] Görres et al. *Phys. Rev. C* to be published.
[34] Garrett J 1992 *Contribution to this Conference.*